ICC 2021 - IEEE International Conference on Communications,14-23 June 2021, Montreal, Canada
DOI: 10.1109/ICC42927.2021.9500720

A Frequency Domain View on Diffusion-based Molecular Communication Channels

Yu Huang[†‡], Fei Ji[†], Miaowen Wen[†], Yuankun Tang[†], Xuan Chen[†], and Weisi Guo[‡]
[†]School of Electronic and Information Engineering, South China University of Technology, China
[‡]School of Aerospace, Transport, and Manufacturing, Cranfield University, U.K.
Email: ee06yuhuang@mail.scut.edu.cn, {eefeiji, eemwwen}@scut.edu.cn,
{eeyktang,eechenxuan}@mail.scut.edu.cn, weisi.guo@cranfield.ac.uk

***Abstract*—Molecular communication (MC) is an emerging communication paradigm, where the information is carried via the patterns of molecules that are mainly governed by the diffusion process. Current MC literature concentrates on the time-domain analysis, while the signal analysis in other domains may facilitate the MC research. To this end, this paper performs the frequency-domain analysis by deriving the frequency response of the diffusion-based MC channels, manifesting an explicitly low-compass characteristic. The energy of the channel impulse response in the diffusion-based MC is also derived, and the corresponding bandwidth definition is proposed, which determines the sampling frequency for the one-shot diffusive channel impulse response in MC. The results in this work lay the foundation for the frequency-domain signal processing in diffusion-based MC channels.**

***Index Terms*—molecular communication, frequency response, energy, bandwidth, sampling.**

I. Introduction

A wide range of organisms uses the molecules as the information carrier for message transmission, and this mechanism is known as MC from a communication perspective. The time-domain analysis of MC is the most common in the literature [1], [2]. MC consists of three basic blocks, namely, transmitter, channel, and receiver. The information in MC transmitter is generally modulated in terms of molecular concentration and type, namely, concentration shift keying (CSK) and molecular shift keying [3], [4]. On-off keying is an energy-efficient CSK modulation scheme, where both release and silence states are used to convey information [5]. The diffusion-based channel is one of the most popular channels in MC research [6], where the molecular concentration signals, i.e., information molecules, are governed by the random diffusion mechanism. The sampled signal at receiver is therefore corrupted by both the inter-symbol interference (ISI) and the signal-dependent counting noise due to the stochastic channel characteristics [7], [8]. Finally, the receiver uses the detection algorithms to recover transmitted signals [9]. The viterbi-like algorithm that alleviates the computationally cumbersome search dimension was studied in [10], and some differential detection methods without updating the detection threshold were proposed in [11], [12]. To get rid of the synchronization and lower the structure complexity, a clock-free receiver was designed in [13]. Furthermore, the signal feature in MC can be exploited, achieving the non-coherent detection without channel information [14].

Except for the amplitude and type, the frequency component has been recognized as a dimension to carry the information of in MC, where the frequency shift keying (FSK) was studied [3], and such mechanism naturally exists in the biological calcium signaling [15]. The robustness of the frequency modulation in a calcium signaling system against noises is studied in [16], where the fast Fourier transform converts the time domain received signal to the frequency domain, and the spectral analysis offers an intuitive explanation on the noise impact. As the enzymatic circuit displays the frequency selective behavior, it was envisioned to be the FSK decoder for MC [17]. An oscillating transmitter generated different longitudinal waves, realizing the possibility of bandpass modulation in MC [18], where the frequency demultiplexing was successfully achieved by recovering the modulated signal from the multiplexed signal. Furthermore, inspired by the optical communication technique, the orthogonal frequency division multiplexing (OFDM) concept was presented for MC in [19]. The inverse fast Fourier transform modulates the signal in OFDM based MC, and the frequency selective channel can be transformed to the parallel channel, such that the ISI can be completely removed with a proper length of cyclic prefix.

The frequency-domain explanation of MC has been first proposed in an early work [20], as the Fourier transform of CIR provided an intuitive explanation of the system transfer function as multiplication operation rather than convolution operation is used, and the bandwidth was quantified via numerical results in [20]. Following the time-frequency analysis of the end-to-end model in [20], the noise characteristics were studied in [7]. Moreover, the pulses with different frequency-domain characteristics were compared in [21], and spike-like pulse with short interval was regarded as a satisfactory shaping strategy through the numerical simulation. In [22], the transfer function of the MC channel with only diffusion effect was derived, based on which the pulse shaping strategy was designed via the inverse Laplace transform. The simulated frequency response of a diffusion-based MC signal showed that the low-frequency components contain most of the signal energy [23], where the rectangular wave was used as the input signal. Specific initial and boundary conditions were

assumed in [24] to derive the MC channel related to the viral propagation. The corresponding frequency response was recognized to facilitate the synchronization and the choice of sampling frequency. Overall, frequency-domain analysis plays a significant role in MC research. Yet, there is no literature related to its rigorous derivation. Against this background, this paper fills such research gap, as the frequency response of diffusion-based CIR is derived for the first time.

The remainder of this paper is organized below. Section II reviews the MC signal characteristics in the time domain. In Section III, we present frequency-domain analysis for MC signals, where the frequency response, energy in the frequency domain, concepts of bandwidth, and sampling frequency in MC are derived. Then, the numerical results are displayed in in Section IV. Finally, the conclusion of this work is drawn, and the future research direction is foreseen in Section V.

II. Time domain System Model

The MC system consists of three fundamental parts, i.e., transmitter, channel, and receiver. The transmitter first sends the information by releasing molecules into the channel, governed by the diffusion mechanism. Finally, the receiver samples the molecular signal, and then decodes it via detection methods. For intuitive explanation, the block diagram of an end-to-end MC system is depicted in Fig. 1. In this paper, the molecular signal is represented by the concentration of molecules. The transmitter is regarded as a point source in the origin of the coordinate, a three-dimensional (3D) communication channel with infinite space is considered, and the receiver has a spherical shape with radius r.

The collision of the molecules causes their random movement, known as the Brownian motion or diffusion, and such diffusion dominates in the micro-scale environment. The diffusion effect is assumed to be inevitable in this paper. The diffusion coefficient determines the dispersion scale of diffusion and has the following form as

$$D = \frac{k_B T}{6\pi\eta R}, \tag{1}$$

where $k_B = 1.38 \times 10^{-23}$J/K is the Boltzmann's constant, T refers to the temperature, η is the dynamic viscosity of the fluid, and R represents the radius of the information molecule [6]. When only the diffusion is considered, such channel is referred to as the free diffusion channel, where the spatiotemporal distribution of the molecular concentration obeys Fick's second law as

$$\frac{\partial c(\mathbf{d},t)}{\partial t} = D\nabla^2 c(\mathbf{d},t), \tag{2}$$

where $c(\mathbf{d},t)$ is the molecular concentration located in the space vector $\mathbf{d}$ at sampling time t, and ∇^2 is the Laplace operator, given by $\nabla^2 = \frac{\partial^2}{\partial x^2} + \frac{\partial^2}{\partial y^2} + \frac{\partial^2}{\partial z^2}$ in the three dimensional Cartesian coordinates. When an impulsive transmission is released by transmitter at time $t = 0$, the initial condition is given by

$$c(\mathbf{0}, t \to 0) = Q\delta(\mathbf{d}), \tag{3}$$

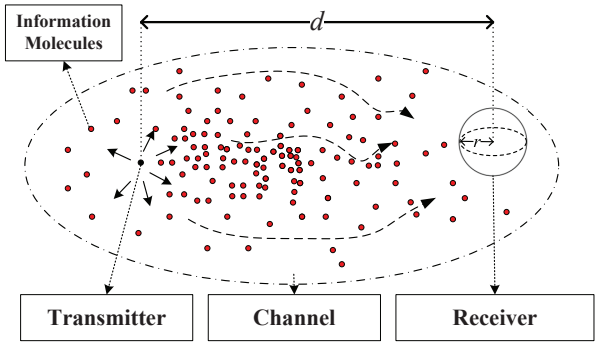

Fig. 1. Diagram of an end-to-end MC system.

where Q is the number of the information molecules per impulse, and $\delta(\cdot)$ is the Dirac function. Besides, the concentration vanishes at the infinitely far distance from the transmitter, which corresponds to the boundary condition as

$$c(\|\mathbf{d}\| \to \infty, t) = 0. \tag{4}$$

When the receiver is situated at $\boldsymbol{d}$, and $\|\boldsymbol{d}\| \gg r$, it has uniform concentration inside [25]. Based on the preceding initial and boundary conditions in (3) and (4), the molecular concentration in (2) yields

$$c(\mathbf{d},t) = \frac{Q}{(4\pi D t)^{\frac{3}{2}}} \exp\left(-\frac{\|\boldsymbol{d}\|^2}{4Dt}\right). \tag{5}$$

By solving the partial derivative of (5) with respect to time to zero, i.e.,

$$\frac{\partial c(\mathbf{d},t)}{\partial t} = 0, \tag{6}$$

the peak concentration arrival time in the free diffusion channel is derived as

$$t_p = \frac{\|\boldsymbol{d}\|^2}{6D}. \tag{7}$$

In this paper, the CIR is defined as the impact of a single information molecule on the receiver, which can be deemed as a scaled version of the concentration signal with bit-1 transmission. When both transmitter and receiver are immobile and the chanel environment is steady, we have fixed $\boldsymbol{d}$ and constant D. Then, under the assumption that $\|\boldsymbol{d}\| \gg r$, the CIR with respect to time is defined as

$$h(t) = \frac{c(\mathbf{d},t)}{Q} = \gamma \frac{\exp\left(-\frac{\alpha}{t}\right)}{t^{\frac{3}{2}}}, \tag{8}$$

where we have

$$\alpha = \frac{\|\boldsymbol{d}\|^2}{4D}, \quad \gamma = \frac{1}{(4\pi D)^{\frac{3}{2}}}, \tag{9}$$

for ease of exposition in the following derivation.

III. Frequency-domain Analysis

The previous section reviews the molecular concentration signal via diffusion from the time domain, while this section concerns its frequency-domain analysis. Channel frequency response is the Fourier transform of the time-domain CIR, which plays an important role in communication systems. The channel energy is obtained over the whole frequency range, and the definition of bandwidth as well as sampling frequency is proposed.

A. Frequency Response

Proposition 1: $h(t)$ is an absolutely integrable function when both transmission distance $\|\boldsymbol{d}\|$ and diffusion coefficient D are finite, and the absolute integration of CIR is given by

$$\int_{-\infty}^{\infty} |h(t)|dt = \frac{1}{4\pi\|\boldsymbol{d}\|D}. \tag{10}$$

Proof: See Appendix A. ∎

Thus, $h(t)$ has its Fourier transform, which is typically referred to as the frequency response for free diffusion channels, given by

$$\begin{aligned} H(\omega) &= \int_{-\infty}^{\infty} h(t) \exp\left(-j\omega t\right) dt \\ &= \frac{1}{4\pi\|\boldsymbol{d}\|D} \exp(-\|\boldsymbol{d}\|\sqrt{\frac{j\omega}{D}}). \end{aligned} \tag{11}$$

Proof: See Appendix B. ∎

Given (11), the amplitude of the frequency response is

$$|H(\omega)| = \frac{1}{4\pi\|\boldsymbol{d}\|D} \exp\left(-\|\boldsymbol{d}\|\sqrt{\frac{\omega}{2D}}\right), \tag{12}$$

and the phase component is

$$\angle H(\omega) = -\|\boldsymbol{d}\|\sqrt{\frac{\omega}{2D}}. \tag{13}$$

Remark 1: The results in (12) and (13) show that both the amplitude and phase depend on the channel parameters $\|\boldsymbol{d}\|$ and D.

The partial derivatives of the amplitude and phase with respect to frequency are given by

$$\frac{\partial|H(\omega)|}{\partial\omega} = -\gamma\sqrt{\frac{\pi}{2\omega}} \exp(-\sqrt{2\alpha\omega}), \tag{14}$$

and

$$\frac{\partial\angle H(\omega)}{\partial\omega} = -\sqrt{\frac{\alpha}{2\omega}}, \tag{15}$$

respectively.

Remark 2: From (14) and (15), it can be found that when $\omega \geq 0$, the amplitude and phase of the frequency response monotonically decrease with the frequency component ω. The diffusion based MC system is, thus, a low-pass channel in the frequency domain.

B. CIR Energy

The energy spectrum density of the desired signal is defined as

$$S_c(w) = |H(\omega)|^2, \tag{16}$$

whose integral over the frequency is the signal energy in the form

$$\frac{1}{2\pi}\int_{-\infty}^{\infty} S_c(w)d\omega = \frac{1}{16\pi^3\|\boldsymbol{d}\|^4 D}. \tag{17}$$

Proof: See Appendix C. ∎

The Parseval's theorem states that the frequency-domain energy equals the time-domain energy. Against this background, an alternative way is to obtain the energy in the time domain as below

$$\frac{1}{2\pi}\int_{-\infty}^{\infty} |H(\omega)|^2 d\omega = \int_{-\infty}^{\infty} |h(t)|^2 dt. \tag{18}$$

Note that the right-hand side of (18) can be derived via similar methods in Appendix A, and an equivalent result as the right-hand side of (17) can be obtained.

Remark 3: The CIR of the MC has finite energy according to (17), and it is inversely proportional to the diffusion coefficient, and the fourth power of transmission distance.

C. Bandwidth and Sampling Frequency

The concentration signal is originally continuous in time, while the digital communication system typically deals with the discrete signal. A discrete sample sequence with a proper sampling frequency is necessary to recover an analog signal with a finite bandwidth. Here, the sampling frequency for one-shot CIR is studied from a frequency-domain perspective.

Since the frequency response of CIR in MC channel shows an exponentially decay over the whole frequency range, the first step is to quantify the cutoff frequency that limits the frequency range, and the signal energy of the truncation over the frequency response from the direct current component (0 Hz) to the cutoff frequency, i.e., bandwidth, should contain most of the energy over the whole frequency range.

We consider the one sided energy spectrum as follows

$$\int_0^{\omega_c} |H(\omega)|^2 d\omega = \eta \int_0^{\infty} |H(\omega)|^2 d\omega, \tag{19}$$

where ω_c is called as the η fractional power containment bandwidth [26], and η represents the portion of the total signal energy, whose value is in the interval of $(0, 1)$. Typically, $\eta = 0.99$, meaning that 99% of the signal power is inside the occupied band.

For the free diffusion channel, we have

$$\omega_c = \frac{D\left(W_{-1}\left(\frac{\eta-1}{\exp(1)}\right)+1\right)^2}{2\|\boldsymbol{d}\|^2}, \tag{20}$$

where $W_k(\cdot)$ is the k-th branch of the Lambert W function [27].

Proof: See Appendix D. ∎

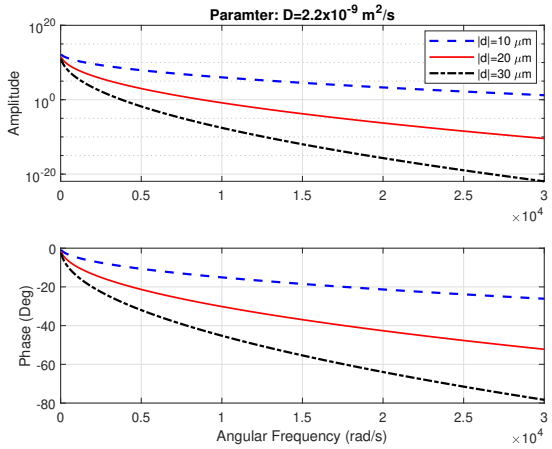

Fig. 2. Amplitude and phase of frequency response with respect to the transmission distance.

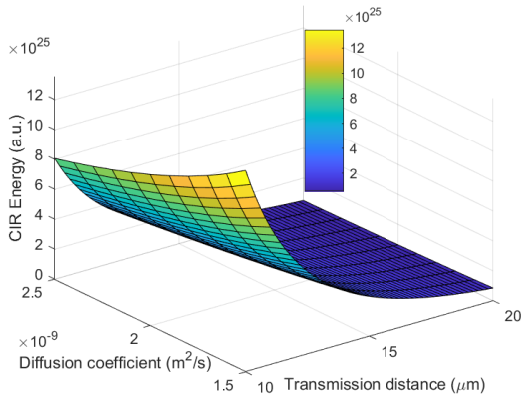

Fig. 3. CIR energy with regard to diffusion coefficient and transmission distance.

According to the Nyquist theorem, the sampling frequency should satisfy

$$\frac{\omega_c}{\pi} \leq F_s < \infty. \tag{21}$$

Note that the result given in (21) is for the information recovery of a one-shot concentration signal, which can be used for channel and distance estimation applications [28].

IV. Numerical Results

The frequency response is shown in Fig. 2. We observe that the amplitude of the frequency response, given by (12), monotonically decreases with the increasing angular frequency. Hence, the free diffusion MC channel has the low-pass feature in the frequency domain. The phase component follows a similar trend as the amplitude component does, decaying with the increase of angular frequency. Furthermore, Fig. 2 depicts the effect of transmission distance on frequency response. We find that the longer the transmission distance, the more rapid decline of both amplitude and phase components along the angular frequency, which is reasonable as the increase of transmission distance leads to higher path-loss.

Figure 3 plots the relationship between the energy of CIR of any unit (a. u.) and its parameters, namely, diffusion coefficient and transmission distance. Clearly, the trend in Fig. 3 obeys the result given in (17) as the energy of CIR decays with increasing of either the distance or the diffusion coefficient.

Figure 4 considers the one-shot transmission, and the relationship between sampling frequency and the energy portion η that first appears in (19), is revealed. The sampling frequency in Fig. 4 is $F_s = \frac{\omega_c}{\pi}$, and the expression of ω_c is derived in (20). The original signal is set as the benchmark to compare with the simulation results with different η values, and it is obtained via an extremely high sampling frequency, which may not be available in practice. Explicitly, the greater η, the better signal recovery. It can be found that when $\eta = [0.5, 0.7, 0.9]$, the signal can not be well recovered since the peak value of the original signal is not sampled due to the low sampling

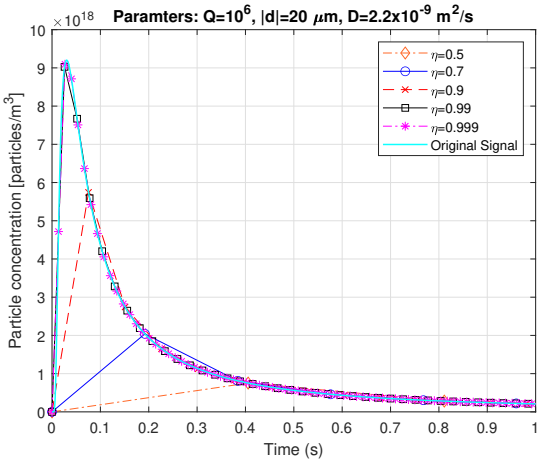

Fig. 4. One-shot concentration signal with different sampling frequencies with regard to the η values.

frequency, which may cause the estimation error of channel and distance. The signal can be almost regenerated when the peak value is sampled in the scenarios of $\eta = 0.99$ and $\eta = 0.999$. However, such large η values indicate a fast sampling frequency, which is a challenging task for the nano-scale receiver due to its size constraint. Thus, the trade-off between sampling frequency and the recovery performance should be considered in the MC system. Furthermore, such sampling frequency is proposed for one-shot transmission instead of the consecutive transmission.

V. Conclusion

While MC has been thoroughly researched in the time domain, its frequency-domain analysis brings new insights. This paper studied the frequency response for the diffusion-based MC system, which intuitively shows the low-pass characteristics. The CIR was proved to have finite energy. From the results in this work, the research in MC can be further extended to the frequency domain.

ACKNOWLEDGMENTS

The works of Y. Huang, F. Ji, M. Wen, Y. Tang, and X. Chen were supported in part by the National Natural Science Foundation of China under Grant 61871190, in part by the Key Program of Marine Economy Development (Six Marine Industries) Special Foundation of Department of Natural Resources of Guangdong Province (GDNRC [2020]009), in part by the Natural Science Foundation of Guangdong Province under Grant 2018B030306005, in part by the Pearl River Nova Program of Guangzhou under Grant 201806010171, and in part by the Fundamental Research Funds for the Central Universities under Grant 2019SJ02. The work of Y. Huang is funded by China Scholarship Council No. 201906150032.

APPENDIX A
PROOF OF PROPOSITION 1

In the free diffusion channel, the integration of $|h(t)|$ over the whole time region is given by

$$\begin{aligned}\int_{-\infty}^{\infty}|h(t)|dt &= \int_{0}^{\infty}h(t)dt \\ &= \gamma\int_{0}^{\infty}\exp\left(-\frac{\alpha}{t}\right)\left(\frac{1}{t}\right)^{\frac{3}{2}}dt \\ &\overset{t=\frac{\alpha}{u^2}}{=} 2\gamma\sqrt{\frac{1}{\alpha}}\int_{0}^{\infty}\exp(-u^2)du \\ &= \gamma\sqrt{\frac{\pi}{\alpha}}\operatorname{erf}(\infty),\end{aligned} \tag{22}$$

Given $\lim_{x\to\infty}\operatorname{erf}(x)=1$ and (9), (22) can be re-written as

$$\int_{-\infty}^{\infty}|h(t)|dt = \frac{1}{4\pi\|\boldsymbol{d}\|D}. \tag{23}$$

In light of (23), when both $\|\boldsymbol{d}\|$ and D are finite, the integration of CIR over time axis converges to a finite value $\frac{1}{4\pi\|\boldsymbol{d}\|D}$ when time approaches to the infinity. In this scenario, $h(t)$ is proved to be an absolutely integrable function.

APPENDIX B
FREQUENCY RESPONSE OF CIR

The frequency response of CIR is the Fourier transform of (8), given by

$$H(\omega) = \int_{-\infty}^{\infty}h(t)\exp\left(-j\omega t\right)dt. \tag{24}$$

For ease of exposition, let $\beta = j\omega$, and (24) can be expanded as

$$\begin{aligned}H(\omega) =&\gamma\int_{0}^{\infty}\frac{\exp\left(-\frac{\alpha}{t}-\beta t\right)}{t^{\frac{3}{2}}}dt \\ =&\gamma\int_{0}^{1}\frac{\exp\left(-\sqrt{\alpha\beta}(\frac{1}{\sqrt{\frac{\beta}{\alpha}}t}+\sqrt{\frac{\beta}{\alpha}}t)\right)}{t^{\frac{3}{2}}}dt \\ &+\gamma\int_{1}^{\infty}\frac{\exp\left(-\sqrt{\alpha\beta}(\frac{1}{\sqrt{\frac{\beta}{\alpha}}t}+\sqrt{\frac{\beta}{\alpha}}t)\right)}{t^{\frac{3}{2}}}dt.\end{aligned} \tag{25}$$

When t is in the interval of $[0,1)$, we can have the substitution as $e^{-u}=\sqrt{\frac{\beta}{\alpha}}t$; when t lies in the interval of $[1,\infty)$, letting $e^{u}=\sqrt{\frac{\beta}{\alpha}}t$,

$$\begin{aligned}H(\omega) =&\gamma\sqrt[4]{\frac{\beta}{\alpha}}\int_{0}^{\infty}\exp\left(-\sqrt{\alpha\beta}(e^{u}+e^{-u})\right)e^{\frac{u}{2}}du \\ &+\gamma\sqrt[4]{\frac{\beta}{\alpha}}\int_{0}^{\infty}\exp\left(-\sqrt{\alpha\beta}(e^{-u}+e^{u})\right)e^{-\frac{u}{2}}du \\ =&2\gamma\sqrt[4]{\frac{\beta}{\alpha}}\int_{0}^{\infty}\exp\left(-2\sqrt{\alpha\beta}(\frac{e^{-u}+e^{u}}{2})\right)\frac{e^{\frac{u}{2}}+e^{-\frac{u}{2}}}{2}du \\ =&2\gamma\sqrt[4]{\frac{\beta}{\alpha}}\int_{0}^{\infty}\exp\left(-2\sqrt{\alpha\beta}\cosh(u)\right)\cosh\left(\frac{u}{2}\right)du \\ =&2\gamma\sqrt[4]{\frac{\beta}{\alpha}}K_{\frac{1}{2}}(2\sqrt{\alpha\beta}),\end{aligned} \tag{26}$$

where $K_m(x)$ is the modified Bessel function of the second kind (Macdonald function), given by [29, Eq. 10.32.9] as

$$K_m(z) = \int_{0}^{\infty}\exp\big(-z\cosh(x)\big)\cosh(mx)dx, \tag{27}$$

for $\angle z < \frac{\pi}{2}$. The modified spherical Bessel function $k_m(z)$ of order m and argument z has an explicit form, which can replace the modified Bessel function given in (27).

The result of [29, Eq. 10.49.12] shows the relationship between the modified spherical Bessel function and the modified Bessel function as

$$\begin{aligned}k_m(z) &= \sqrt{\frac{\pi}{2z}}K_{\pm(m+\frac{1}{2})}(z) \\ &= \frac{\pi}{2}\exp(-z)\sum_{k=0}^{m}\frac{a_k(m+\frac{1}{2})}{z^{k+1}},\end{aligned} \tag{28}$$

where we have

$$a_k(m+\frac{1}{2}) = \begin{cases}\frac{(m+k)!}{2^k k!(m-k)!}, & k=0,1,\ldots,m \\ 0, & k=m+1,m+2,\ldots.\end{cases} \tag{29}$$

By substituting (29) into (28), we can obtain $k_0(z) = \frac{\pi}{2z}\exp(-z)$. In light of this, the frequency response has a closed-form expression below

$$\begin{aligned}H(\omega) &= 4\gamma\sqrt{\frac{\beta}{\pi}}k_0(2\sqrt{\alpha\beta}) \\ &= \frac{1}{4\pi\|\boldsymbol{d}\|D}\exp\left(-\|\boldsymbol{d}\|\sqrt{\frac{j\omega}{D}}\right).\end{aligned} \tag{30}$$

APPENDIX C
SIGNAL ENERGY IN THE FREQUENCY DOMAIN

For the free diffusion channel, we have the frequency-domain energy in the single side band as

$$\frac{1}{\pi}\int_{0}^{\infty}|H(\omega)|^2d\omega = \frac{\gamma^2}{\alpha}\int_{0}^{\infty}\exp\left(-2\sqrt{2\alpha\omega}\right)d\omega. \tag{31}$$

Then (31) can be re-written as

$$\frac{1}{\pi}\int_0^\infty |H(\omega)|^2 = \frac{\gamma^2}{4\alpha^2}\int_0^\infty u\exp(-u)du = \frac{1}{16\pi^3\|\boldsymbol{d}\|^4 D}, \tag{32}$$

where we have $u = 2\sqrt{2\alpha\omega}$.

APPENDIX D
BANDWIDTH OF FREE DIFFUSION CHANNEL

Based on the integrals in (32) of Appendix C, (19) can be rearranged as

$$\frac{2\sqrt{2\alpha\omega_c}+1}{\exp(2\sqrt{2\alpha\omega_c})} = 1-\eta. \tag{33}$$

By multiplying $-\exp(-1)$ on both sides of (33), it has the following form, i.e.,

$$\frac{-2\sqrt{2\alpha\omega_c}-1}{\exp(2\sqrt{2\alpha\omega_c}+1)} = \frac{\eta-1}{\exp(1)}. \tag{34}$$

Define $x = -2\sqrt{2\alpha\omega_c}-1$ and $z = \frac{\eta-1}{\exp(1)}$. Then (34) is converted to the following form as

$$x\exp(x) = z, \tag{35}$$

where the solution for x is the Lambert W function $W_k(z)$, where the subscript k indicates the k-th branch of the Lambert W function [27]. Note that in (35), z is only valid over the interval $[-\exp(-1),\infty)$. When z is a real value in the interval $[-\exp(-1),0)$, x has two possible values, $W_0(z)\in[-1,0)$ or $W_{-1}(z)\in(-\infty,-1]$, while the solution is $W_0(z)$ over the interval $[0,\infty)$.

Here, $x = -2\sqrt{2\alpha\omega_c}-1 < -1$ and $-\exp(-1) < z = \frac{\eta-1}{\exp(1)} < 0$. Against this background, the solution for x in (35) is

$$x = -2\sqrt{2\alpha\omega_c}-1 = W_{-1}\left(\frac{\eta-1}{\exp(1)}\right). \tag{36}$$

Based on (9), the corresponding bandwidth with respect to the proportion value η has the form of

$$\omega_c = \frac{D\left(W_{-1}\left(\frac{\eta-1}{\exp(1)}\right)+1\right)^2}{2\|\boldsymbol{d}\|^2}. \tag{37}$$

REFERENCES

[1] T. Nakano, A. W. Eckford, and T. Haraguchi, *Molecular Communication*. Cambridge University Press, 2013.

[2] N. Farsad *et al.*, "A comprehensive survey of recent advancements in molecular communication," *IEEE Commun. Survey & Tut.*, vol. 18, no. 3, pp. 1887–1919, third quarter 2016.

[3] M. U. Mahfuz, D. Makrakis, and H. T. Mouftah, "On the characterization of binary concentration-encoded molecular communication in nanonetworks," *Nano Commun. Netw.*, vol. 1, no. 4, pp. 289 – 300, 2010.

[4] M. S. Kuran, H. B. Yilmaz, T. Tugcu, and I. F. Akyildiz, "Modulation techniques for communication via diffusion in nanonetworks," in *Proc. IEEE International Conf. on Commun. (ICC)*, Kyoto, Japan, June 2011, pp. 1–5.

[5] L. Shi and L. L. Yang, "Error performance analysis of diffusive molecular communication systems with on-off keying modulation," *IEEE Trans. Mol. Biol. Multi-Scale Commun.*, vol. 3, no. 4, pp. 224–238, Dec. 2017.

[6] V. Jamali *et al.*, "Channel modeling for diffusive molecular communication—a tutorial review," *Proc. IEEE*, vol. 107, no. 7, pp. 1256–1301, July 2019.

[7] M. Pierobon and I. F. Akyildiz, "Diffusion-based noise analysis for molecular communication in nanonetworks," *IEEE Trans. Signal Process.*, vol. 59, no. 6, pp. 2532–2547, June 2011.

[8] B. Tepekule *et al.*, "ISI mitigation techniques in molecular communication," *IEEE Trans. Mol. Biol. Multi-Scale Commun.*, vol. 1, no. 2, pp. 202–216, June 2015.

[9] D. Kilinc and O. B. Akan, "Receiver design for molecular communication," *IEEE J. Sel. Areas Commun.*, vol. 31, no. 12, pp. 705–714, Dec. 2013.

[10] Y. Tang *et al.*, "Molecular type permutation shift keying for molecular communication," *IEEE Trans. Mol. Biol. Multi-Scale Commun.*, vol. 6, no. 2, pp. 160–164, Nov. 2020.

[11] H. Yan, G. Chang, Z. Ma, and L. Lin, "Derivative-based signal detection for high data rate molecular communication system," *IEEE Commun. Lett.*, vol. 22, no. 9, pp. 1782–1785, Sept. 2018.

[12] Y. Huang *et al.*, "A rising edge-based detection algorithm for MIMO molecular communication," *IEEE Wireless Commun. Lett.*, vol. 9, no. 4, pp. 523–527, Apr. 2020.

[13] Q. Li, "The clock-free asynchronous receiver design for molecular timing channels in diffusion-based molecular communications," *IEEE Trans. Nanobiosci.*, vol. 18, no. 4, pp. 585–596, Oct. 2019.

[14] Z. Wei, W. Guo, B. Li, J. Charmet, and C. Zhao, "High-dimensional metric combining for non-coherent molecular signal detection," *IEEE Trans. Commun.*, vol. 68, no. 3, pp. 1479–1493, Mar. 2020.

[15] M. J. Berridge, "The AM and FM of calcium signalling," *Nature*, vol. 386, p. 759–760, Apr. 1997.

[16] P. He *et al.*, "Stochastic channel switching of frequency-encoded signals in molecular communication networks," *IEEE Commun. Lett.*, vol. 22, no. 2, pp. 332–335, Feb. 2018.

[17] C. T. Chou, "Molecular circuits for decoding frequency coded signals in nano-communication networks," *Nano Commun. Netw.*, vol. 3, no. 1, pp. 46 – 56, 2012.

[18] W. Guo, B. Li, S. Wang, and W. Liu, "Molecular communications with longitudinal carrier waves: Baseband to passband modulation," *IEEE Commun. Lett.*, vol. 19, no. 9, pp. 1512–1515, Sept. 2015.

[19] M. Damrath, J. J. Koshy, and P. A. Hoeher, "Application of OFDM in diffusion-based molecular communication," *IEEE Trans. Mol. Biol. Multi-Scale Commun.*, vol. 3, no. 4, pp. 254–258, Dec. 2017.

[20] M. Pierobon and I. F. Akyildiz, "A physical end-to-end model for molecular communication in nanonetworks," *IEEE J. Sel. Areas Commun.*, vol. 28, no. 4, pp. 602–611, May 2010.

[21] N. Garralda, I. Llatser, A. Cabellos-Aparicio, E. Alarcón, and M. Pierobon, "Diffusion-based physical channel identification in molecular nanonetworks," *Nano Commun. Networks*, vol. 2, no. 4, pp. 196–204, Dec. 2011.

[22] S. Wang, W. Guo, and M. D. McDonnell, "Transmit pulse shaping for molecular communications," in *Proc. IEEE Conf. on Comput. Commun. Workshops (INFOCOM WKSHPS)*, Toronto, Canada, Apr. 2014, pp. 209–210.

[23] B. Li *et al.*, "CSI-independent non-linear signal detection in molecular communications," *IEEE Trans. Signal Process.*, vol. 68, pp. 97–112, Jan. 2020.

[24] M. Khalid *et al.*, "Modeling of viral aerosol transmission and detection," *IEEE Trans. Commun.*, vol. 68, no. 8, pp. 4859–4873, Aug. 2020.

[25] A. Noel, K. C. Cheung, and R. Schober, "Using dimensional analysis to assess scalability and accuracy in molecular communication," in *Proc. IEEE International Conf. on Commun. Workshops (ICC)*, Budapest, Hungary, June 2013, pp. 818–823.

[26] F. Amoroso, "The bandwidth of digital data signal," *IEEE Commun. Mag.*, vol. 18, no. 6, pp. 13–24, Nov. 1980.

[27] F. Chapeau-Blondeau and A. Monir, "Numerical evaluation of the lambert W function and application to generation of generalized gaussian noise with exponent 1/2," *IEEE Trans. Signal Process.*, vol. 50, no. 9, pp. 2160–2165, Sept. 2002.

[28] M. J. Moore, T. Nakano, A. Enomoto, and T. Suda, "Measuring distance from single spike feedback signals in molecular communication," *IEEE Trans. Signal Process.*, vol. 60, no. 7, pp. 3576–3587, July 2012.

[29] F. W. J. Olver, D. W. Lozier, R. F. Boisvert, and C. W. Clark, *NIST Handbook of Mathematical Functions*. Cambridge University Press, 2010.

2021-08-06

A frequency domain view on diffusion-based molecular communication channels

Huang, Yu

IEEE

Huang Y, Ji F, Wen M, et al., (2021) A frequency domain view on diffusion-based molecular communication channels. In: ICC 2021 - IEEE International Conference on Communications,14-23 June 2021, Montreal, Canada

https://doi.org/10.1109/ICC42927.2021.9500720